JOURNAL OF VIROLOGY, Aug. 2002, p. 7651–7660 Vol. 76, No. 15
0022-538X/02/$04.00+0 DOI: 10.1128/JVI.76.15.7651–7660.2002

Virus-Mediated Transduction of Murine Retina with Adeno-Associated Virus: Effects of Viral Capsid and Genome Size

Grace S. Yang,[1] Michael Schmidt,[2] Ziying Yan,[3] Jonathan D. Lindbloom,[4] Thomas C. Harding,[5] Brian A. Donahue,[5] John F. Engelhardt,[3] Robert Kotin,[2] and Beverly L. Davidson[4,6,7]*

Program in Gene Therapy, Departments of Otolaryngology,[1] Internal Medicine,[4] Neurology,[6] Physiology and Biophysics,[7] and Anatomy and Cell Biology,[3] University of Iowa College of Medicine, Iowa City, Iowa; National Heart, Lung, and Blood Institute, Bethesda, Maryland[2]; and Cell Genesys Inc., Foster City, California[5]

Received 22 January 2002/Accepted 18 April 2002

Gene therapy vectors based on adeno-associated viruses (AAVs) show promise for the treatment of retinal degenerative diseases. In prior work, subretinal injections of AAV2, AAV5, and AAV2 pseudotyped with AAV5 capsids (AAV2/5) showed variable retinal pigmented epithelium (RPE) and photoreceptor cell transduction, while AAV2/1 predominantly transduced the RPE. To more thoroughly compare the efficiencies of gene transfer of AAV2, AAV3, AAV5, and AAV6, we quantified, using stereological methods, the kinetics and efficiency of AAV transduction to mouse photoreceptor cells. We observed persistent photoreceptor and RPE transduction by AAV5 and AAV2 up to 31 weeks and found that AAV5 transduced a greater volume than AAV2. AAV5 containing full-length or half-length genomes and AAV2/5 transduced comparable numbers of photoreceptor cells with similar rates of onset of expression. Compared to AAV2, AAV5 transduced significantly greater numbers of photoreceptor cells at 5 and 15 weeks after surgery (greater than 1,000 times and up to 400 times more, respectively). Also, there were 30 times more genome copies in eyes injected with AAV2/5 than in eyes injected with AAV2. Comparing AAVs with half-length genomes, AAV5 transduced only four times more photoreceptor cells than AAV2 at 5 weeks and nearly equivalent numbers at 15 weeks. The enhancement of transduction was seen at the DNA level, with 50 times more viral genome copies in retinas injected with AAV having short genomes than in retinas injected with AAV containing full-length ones. Subretinal injection of AAV2/6 showed only RPE transduction at 5 and 15 weeks, while AAV2/3 did not transduce retinal cells. We conclude that varying genome length and AAV capsids may allow for improved expression and/or gene transfer to specific cell types in the retina.

Gene transfer to the retina has been accomplished with viral and nonviral vectors (2, 14, 25, 27). Recombinant adeno-associated viruses (AAVs) have been shown to direct long-term expression in multiple tissues, including the central nervous system (2, 9, 11). AAVs are promising vectors for gene therapy in the retina because AAV vectors can infect nondividing cells, are replication defective, and lack viral coding sequences that induce immune responses to viral translation products (31).

Six AAV serotypes have been described (AAV1 to -6). Their genomes consist of a single strand of DNA approximately 4.7 kb in length, with inverted terminal repeats (ITRs) flanking Rep- and Cap-encoding regions (7, 30). AAV6 likely arose from homologous recombination between AAV1 and AAV2, resulting in a coding region identical to that of AAV1 (37). AAV5 is the most divergent from all other serotypes in sequence and biochemical comparisons. The Rep-encoding regions of AAV2, AAV3, and AAV6 are approximately 90% similar, while those of AAV2 and AAV5 are 67% similar (7). The AAV5 ITR is 58% homologous to the AAV2 ITR; the homology is much lower than that observed with AAV3 and AAV6. The Rep binding motif and terminal resolution sites (TRS) have been found to be critical for the function of the ITR as an origin of viral replication. The TRS is conserved among AAV2, AAV3, and AAV6, but the TRS of these three AAVs are weakly similar to the AAV5 TRS. The high degree of conservation of the Rep genes and ITRs among AAV2, AAV3, and AAV6 allow for a cross complementation among the Rep genes and ITRs of these serotypes (6, 18). In contrast, the Rep gene and ITR of AAV5 fail to cross-complement those of AAV1 to -4 (6).

Vectors constructed from AAV2, AAV3, AAV5, and AAV6 variably transduce different cell lines (18, 30). Pseudotyped AAV6 (AAV2 genome packaged in an AAV6 capsid or AAV2/6) vectors are more efficient than AAV2 in transducing the apical airway epithelium in vitro (18). Relative to AAV2, AAV2/3 and AAV2/6 vectors were less and more efficient, respectively, for transduction of alveoli and airway epithelia (18, 19). AAV2/3 showed improved transduction of smooth muscle cells in the mouse lung (18, 19). AAV5 was found to be more efficient than AAV2 at gene transfer to the apical surface of airway epithelia in vitro and in vivo (40). AAV5 has also been shown to have transduction profiles distinct from those of AAV2 in the ependymal cells lining the ventricles of the central nervous system, cerebral neurons, and muscle in vivo (9, 21).

Transduction efficiency is dependent on viral binding, entry, and postentry processes. The capsid protein sequence shows significant variation among the AAV serotypes (7, 30). Unlike AAV2, AAV 2/6 and AAV5 vectors are not inhibited by heparin (18, 40). The receptors and coreceptors for AAV2 include heparan sulfate proteoglycan, fibroblast growth factor receptor 1, and $\alpha_V\beta5$ integrins (29, 34, 35). It has recently been shown

* Corresponding author. Mailing address: 200 EMRB, University of Iowa College of Medicine, Iowa City, IA 52242. Phone: (319) 353-5511. Fax: (319) 353-5572. E-mail: beverly-davidson@uiowa.edu.

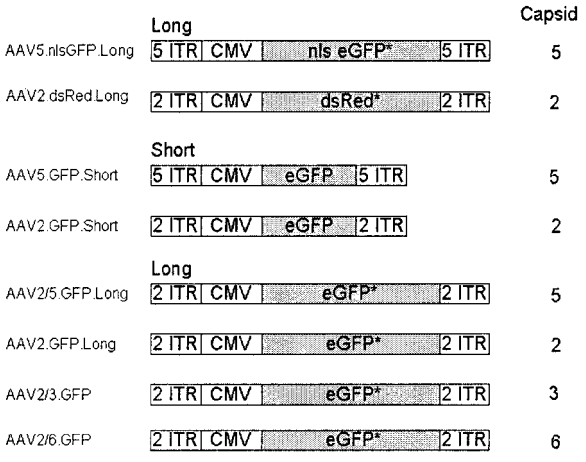

FIG. 1. Cartoon of the AAV vectors used. CMV, CMV promoter and enhancer; nls eGFP, nucleus-targeted eGFP; dsRed, coding sequence for red fluorescent protein; short, total length of vector is 2.3 kb; long, total length of vector is equivalent to that of wild type (4.6 to 5.0 kb). *, eGFP or dsRed coding sequence plus stuffer sequences (see Materials and Methods).

that 2,3-linked sialic acid is a component of the receptor complex for AAV5 (36). AAV2/5 more efficiently infected differentiated airway epithelial cells from the apical surface than AAV2 and allowed for intermediate transgene expression between AAV5 and AAV2 in muscle (21). Interestingly, AAV2 transduced differentiated myocytes more poorly than AAV2/5, despite its higher binding efficiency (12). Thus, AAV2, -3, -5, and -6 may have distinct interactions with host factors in specific entry or postentry processes, and these interactions may affect the conversion of single-stranded vector genomes into transcriptionally active forms.

In the retina, AAV2 has been tested more extensively than the remaining serotypes (1, 2, 4, 15). Subretinal injections of AAV2 in mice consistently transduced retinal pigmented epithelium (RPE) cells and some photoreceptor cells (1, 2, 4, 15). It has recently been shown that subretinal injection of AAV5 and AAV2/5 transduces both RPE and photoreceptor cells, with higher levels of gene expression in the RPE layer (2). Subretinal injection of AAV2/1 transduced mostly the RPE, with fewer positive photoreceptor cells, Müller cells, and cells in the inner nuclear layer (INL) (2). The different host ranges of the various AAV serotypes are important for gene therapy in the eye, as retinal degeneration develops from mutations in genes expressed in specific cell types. However, most of the identified genes causing retinal degeneration are expressed specifically in photoreceptor cells (10). As we move toward clinical use of AAV, it is important to further define the kinetics and efficiency of AAV transduction of photoreceptor cells. In this study, we quantified the effects of AAV capsid and genome length on numbers of photoreceptor cells transduced following subretinal injection.

MATERIALS AND METHODS

Vector production. The plasmids for vector production, listed in Fig. 1, were derived as follows. AAV2.dsRed.Long was produced by using proviral plasmid pAAV2-dsRed and the pDG helper plasmid (16). pAAV2-dsRed was constructed by inserting the *Apa*LI/*Eco*RII fragment of pDsRed-N1 (Clontech) into *Pml*I- and *Sna*BI-digested pMCS2, which provides the AAV2 ITRs. Plasmid pMCS2.7 was derived from pAV2 (24), which was digested with *Sna*B1, which cuts AAV2 once at nucleotide (nt) 4495. A synthetic oligonucleotide with multiple restriction endonuclease recognition sites and a polyadenylation signal was ligated to the blunt ends of the plasmid, and the plasmid was recircularized. This intermediate construct was digested with *Ppu*M1, which cuts twice at within the AAV genome at nt 189 and 349, and also with *Pml*I, which cuts at nt 2448 and 3249. A different polylinker was ligated, and the plasmid was recircularized. pAAV2-dsRed contains, flanked by AAV2 ITRs, sequences of the cytomegalovirus (CMV) immediate-early promoter, the red fluorescent protein (dsRed) coding sequence, simian virus 40 (SV40) poly(A), the SV40 origin, a neomycin resistance cassette, and herpes simplex virus (HSV) thymidine kinase (TK) poly(A).

AAV5.nlsGFP.Long was produced by using proviral plasmid pAAV5-nls-GFP and the pSR449B helper plasmid (33). pAAV5-nls-GFP was constructed by inserting the *Apa*LI/*Eco*RII fragment of pNLS-GFP into *Bgl*II- and *Pvu*II-digested p7D05, a plasmid providing the AAV5 ITRs (32, 33). pAAV5-nls-GFP contains, flanked by the AAV5 ITRs, sequences of the CMV immediate-early promoter, nlsGFP, SV40 poly(A), the SV40 origin, a neomycin resistance cassette, and HSV TK poly(A).

AAV2.GFP.Long was produced by using a proviral plasmid (pcisEGFPori3) and an AAV2 helper plasmid (pAAV-2/Ad) as previously described (11). pcisEGFori3 contains a 4.7-kb AAV component (CMV enhancer and promoter, eGFP, a 2.5-kb cassette containing the β-lactamase and bacterial replication origin, and SV40 poly[A]) flanked by a 2-kb stuffer sequence which was derived from the luciferase gene of the pGL3-basic vector (Promega) (11). AAV2/5.GFP.Long was produced by using a proviral plasmid (pcisEGFPori3), pAV2-Rep, and pAV5-Trans. The AAV5 helper plasmid (pAV5-Trans) and the AAV2 Rep plasmid (pAV2-Rep) were used to package the AAV2 genome into the AAV5 capsid. pAV2-Rep was generated by deleting the AAV2 Cap gene in pAAV/Ad (39).

The AAV2.GFP.Short was produced by using a proviral plasmid (pAV2.CMVeGFP) and pAAV2-2/AD. pAV2.CMVeGFP contains a 1.89-kb eGFP expression cassette (CMV promoter and enhancer, eGFP cDNA and SV40 poly[A]). The total length, including the AAV2 ITRs flanking the cassette, is 2,299 nt (38). AAV5.GFP.Short was produced by using a proviral plasmid (pAV5.CMVeGFP) and pAV5-trans. pAV5.CMVeGFP contains a 1.89-kb eGFP expression cassette (CMV promoter and enhancer, eGFP cDNA, and SV40 poly[A]). The total length, including the AAV5 ITRs, is 2.3 kb.

AAV2/3.GFP and AAV2/6.GFP were prepared by using helper plasmids pRepCap3 and pRepCap6. The AAV2 recombinant genome expressed the GFP gene from the 3-kb cassette of pTRUF5 (CMVie promoter, SV40 SD/SA, and poly[A], TK neo, and bovine growth hormone poly[A]) (23).

AAV5.nlsGFP.Long and AAV2.dsRed.Long were produced in human embryonic kidney 293T cells, and AAV5.GFP.Short, AAV2.GFP.Short, AAV2/5.GFP.Long, and AAV2.GFP.Long were produced in 293 cells, using an adenovirus-free system by cotransfecting AAV vector and helper plasmids. Forty-eight hours after transfection, crude viral lysates were cleared, and the cleared lysates were purified by CsCl centrifugation (8). AAV2/3.GFP and AAV2/6.GFP vectors were prepared in 293 cells by cotransfecting the vector plasmid and helper plasmid pRepCap3 or pRepCap6 (gift from David Russell, University of Washington [30]) by the calcium phosphate method. Cells were then infected with adenovirus Ad5 *dl*312 (an E1A$^-$ mutant) at a multiplicity of infection of 2, and the infection was allowed to proceed for 72 h. Cells were harvested, lysed, and treated with Benzonase (Nycomed) to remove the cellular debris. Cleared cell lysates were fractionated by ammonium sulfate precipitation, and the recombinant AAV virions were isolated on CsCl gradients. The CsCl gradient fractions containing AAV vectors were dialyzed against either sterile phosphate-buffered saline (pH 7.4) containing 0.9 mM $CaCl_2$ and 0.5 mM $MgCl_2$ or against HEPES buffer (20 mM HEPES, 150 mM NaCl, pH 7.8). AAV2/3 and AAV2/6 were heated for 30 min at 56°C to inactivate any residual adenovirus without loss of biological activity (Brian Donahue, unpublished results). The physical titers of the viral stocks were determined by slot blot hybridization against plasmid standards. The infectious titers of the viral stocks were also tested in multiple cell lines. As expected, the infectious unit/particle ratio was dependent on the cell type transduced, reflecting the specific tropism of the distinct capsids. For example, in HeLa cells, primary fetal fibroblasts, IB3 cells, 293 cells, and undifferentiated C2C12 muscle cells, transgene expression was lower (6- to 25-fold) for AAV2/5 than for AAV2. In differentiated C2C12 cells, AAV2/5 had 30-fold higher reporter gene expression than AAV2 (39).

Subretinal injection of rAAV. All animal procedures were approved by the University of Iowa Animal Care and Use Committee. Adult C57BL/6J mice (Jackson Laboratory) between 2 and 4 months of age were anesthetized with

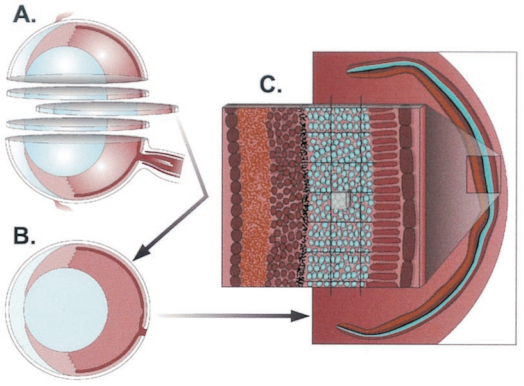

FIG. 2. Stereological analysis utilizing the optical fractionator was performed as schematically depicted to evaluate the efficiency of AAV transduction of murine photoreceptor cells. Eyes were serially sectioned (A) and oriented in such a way that each section contained the anterior and posterior parts of the eye (B). (C) Enlarged area of the retina, depicting the area of interest (blue, photoreceptor cells) and the overlying grid. Within the grid the counting box is shown. To determine the number of transgene-positive photoreceptor cells, the counting box was translated over grid intersections and cells were counted as described in Materials and Methods.

intraperitoneal injections of ketamine-xylazine (ketamine, 100 to 125 mg/kg of body weight; xylazine, 10 to 12.5 mg/kg), pupils were dilated (2.5% phenylephrine HCl, 1 drop; 2% cyclopentolate HCl, 1 drop), and a local anesthetic (0.5% proparacaine HCl; 1 drop) was applied. An ophthalmic operating microscope was used to make an incision slightly behind the ora serrata, and a blunt 33-gauge needle (Hamilton syringe) was inserted through the sclerotomy, delivering 1.5 μl of rAAV suspension per eye into the subretinal space. The delivery of the suspension was confirmed by partial detachment of the retina.

Tissue processing. All mice were injected with an overdose of ketamine-xylazine and transcardially perfused with phosphate-buffered saline, followed by 2% paraformaldehyde. The eyes were enucleated, and corneas were trimmed. The lens and vitreous humor of each eye were removed, and the posterior eye cup was placed in 2% paraformaldehyde for 2 h. The eyes were then infiltrated with acrylamide embedding solution (1.2 M acrylamide, 0.9 mM bisacrylamide, 0.7% *N,N,N′,N′*-tetramethylethylenediamine, 1 mM $MgCl_2$, 1 mM $CaCl_2$) for 2 h and polymerized (acrylamide embedding solution and 2 mM ammonium persulfate). The acrylamide was then trimmed to the size of the posterior eye cup, and the eyes were embedded in OCT (Tissue-Tek). Samples were cut into 10-μm-thick sections in an orientation such that each section included both the anterior and posterior portions of the eye.

Stereological assessment of transduction efficiency. Stereological analysis (Fig. 2) was performed by the optical fractionator technique using the Bioquant software and a motorized x-y-z stage (Applied Scientific Instruments) coupled to a video microscopy system. Systematic random sampling was utilized to analyze each eye. A three-dimensional probe for counting was placed systematically throughout the outer nuclear layer (ONL) of the murine retina. The sum of GFP- or dsRed-positive cells counted with the three-dimensional probe was multiplied by the reciprocal of the fraction of the reference space that was sampled. This gives the total number of transduced photoreceptor cells within each eye.

The scheme utilized was as follows. After a random start section was selected, every 32nd section was selected throughout the entire eye, yielding 9 or 10 sections per eye for analysis. The three-dimensional probe selected was 20 by 20 by 10 μm and was randomly translated over a regular grid of 110 by 110 μm. The precision of the measurement was estimated by determining the coefficient of error using Matheron's quadratic approximation formula (17). All data sets are expressed as means ± standard errors.

Evaluating volume of distribution. Coinjection of viruses allowed for evaluation of differences in distribution. The 9 or 10 sections per eye previously selected for stereology analysis were utilized. With the aid of the Bioquant software, the region within the ONL that included positive cells was outlined and its area was determined. The area was then multiplied by 320 μm, the distance between sections analyzed, and results for all sections were summed for the total volume.

Hirt DNA extraction. Animals were sacrificed, and the retina was removed from the posterior cup of the eye, leaving RPE behind. Samples were homogenized in buffer containing 10 mM Tris (pH 8.0), 10 mM EDTA, 1% sodium dodecyl sulfate, and 1 μl of RNase (DNase free; 10 mg/ml stock; Boehringer Mannheim Biochemicals). After 30 min of incubation at 37°C, proteinase K was added to a final concentration of 1 mg/ml. After incubation at 37°C for 2 h, NaCl was added to a final concentration of 1.1 M and DNA precipitated overnight at 4°C. Samples were then spun at 15,000 × *g* for 30 min at 4°C. Low-molecular-weight Hirt DNA was purified from the supernatant by phenol-chloroform extraction and ethanol precipitation. The final DNA was resuspended in 40 μl of 10 mM TrisCl–1 mM EDTA, pH 8.0, and stored at −20°C.

Quantification of viral genome with real-time PCR. Real-time PCR was performed using the SYBR green I dye (PE Biosystems) with an ABI Prism 7700 sequence detection system. A standard curve was generated with an eGFP-containing plasmid by serial 10-fold dilutions from 10^2 to 10^8 genome copies. Retinal eye samples spiked with known amounts of plasmid were used to determine the theoretical detection limits. All samples were tested in two separate PCR assays and in triplicate for each assay. Primers were selected by using Primer Express software. The sequence of the forward primer is AGTCCGCC CTGAGCAAAGA, and that of the reverse primer is GCGGTCACGAACTCC AGC. The amplicon generated was100 bp. The amplification was performed in 96-well plates in 25-μl reaction mixtures containing 1 μl of sample, 300 nM (each) forward and reverse primer, and SYBR green PCR Master Mix (PE Biosystems). Dissociation curves were generated following each real-time PCR run, and PCR products were electrophoresed through agarose and analyzed to ensure the absence of primer-dimer formation.

Real-time PCR reliability. Reliability of the PCR assays was assessed by using intraclass correlation. The intra-assay correlation was 0.918 (95% confidence interval, 0.825 to 0.934). The interassay correlation was 0.758 (95% confidence interval, 0.537 to 0.852).

Statistical analysis. All statistical calculations were made with SAS/STAT software (version 8; SAS Institute Inc.). The number of GFP- and dsRED-positive photoreceptor cells and the number of genome copies per retina were normalized by log transformation prior to data comparison using two sample *t* tests for equal and unequal variance. The log means were presented as geometric means in the results after back-transformation (antilog).

RESULTS

Coinfection of AAV5.nlsGFP.Long and AAV2.dsRed.Long. In initial studies we assessed the ability of AAV2 and AAV5 to transduce retinal cells following subretinal delivery. A mixture of equivalent particles (1.5×10^7 particles each) of AAV5.nlsGFP.Long and AAV2.dsRed.Long (Fig. 1) was injected for intraeye comparisons, and mice were sacrificed 5 ($n = 9$ eyes), 15 ($n = 6$ eyes), and 31 ($n = 6$ eyes) weeks later. Transgene-positive cells were quantified by stereological methods (Fig. 2). GFP-positive photoreceptor and RPE cells were observed in AAV5.nlsGFP.Long-injected eyes at 5, 15 (not shown), and 31 weeks (Fig. 3). In contrast, dsRed-positive photoreceptor and RPE cells were not observed until week 15. At week 5, AAV5-mediated expression (63,000 ± 17,000 GFP-positive cells) was significantly greater than AAV2 transgene expression (Fig. 4; $P < 0.0001$). By week 15, dsRed expression increased up to a mean of 57,000 ± 7,400 dsRed-positive cells relative to 220,000 ± 32,000 GFP-positive cells ($P = 0.016$). At week 31, mean levels of expression of AAV5 and AAV2 (74,000 ± 19,000 GFP-positive cells versus 6,600 ± 5,000 dsRed-positive cells) were not significantly different ($P = 0.22$). These results indicate that AAV5 and AAV2 transduce photoreceptor and RPE cells in the murine retina. The time course for expression was faster with AAV5 than with AAV2, and more photoreceptor cells were transduced with AAV5. AAV5 reached maximum levels of expression at week 5, the earliest point examined, with expression levels maintained to week 31, the latest time point tested ($P = 0.11$). AAV2 trans-

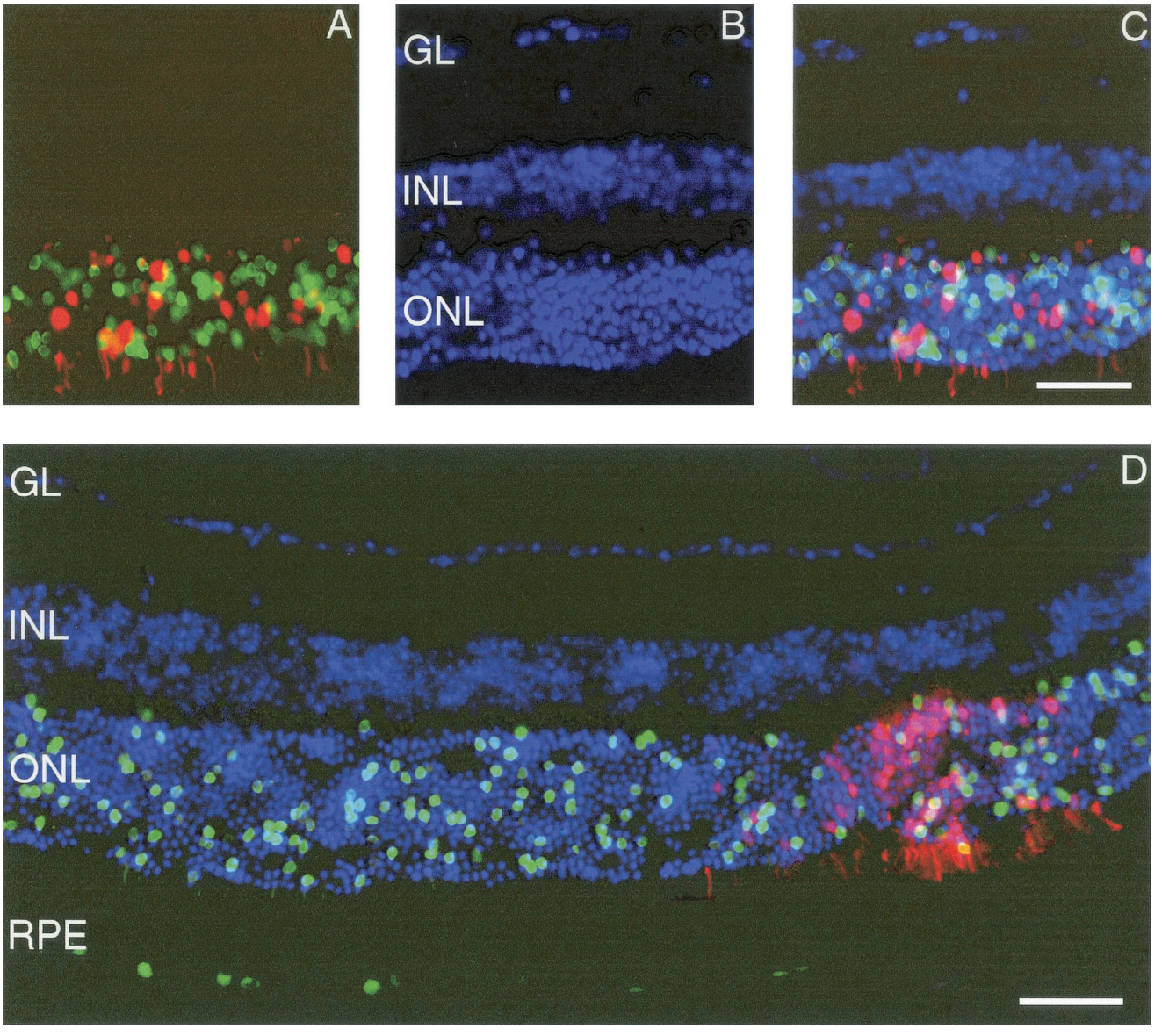

FIG. 3. Murine retina coinfected with AAV5.nlsGFP.Long and AAV2.dsRed.Long 31 weeks after subretinal delivery. (A) nucleus-targeted GFP-positive nuclei and dsRed-positive nuclei and cytoplasm of photoreceptor cells. (B) DAPI (4′,6′-diamidino-2-phenylindole)-positive nuclei in the layers of murine retina. (C) Superimposed images of panels A and B, showing positive nuclei in the ONL. (D) Extent of AAV5- versus AAV2-mediated reporter expression in the ONL and RPE. GL, ganglion layer. Photomicrographs are similar to those taken from retinas harvested 15 weeks after surgery. Bars, 50 μm.

gene expression was not evident until after week 5 but remained stable once maximum levels of expression were attained ($P = 0.24$ for 15 and 31 weeks).

We next compared the volumes of transduction of the two viruses. At week 15, evaluation of GFP and dsRED expression in six out of six eyes showed that AAV5 transduced a 1.5- to 2-fold-greater volume of the retina than AAV2 (Fig. 5A). The results at week 31 were consistent in four out of five eyes (Fig. 5B). One eye showed no dsRed expression and was not further analyzed.

Separate infection of AAV5.nlsGFP.Long and AAV2.dsRed.Long. Prior work demonstrated that dsRed matures slowly relative to GFP (48 h in yeast two-hybrid assays) and fluoresces green during maturation (3). Although the time course for our study (greater than 5 weeks) was well beyond that required for dsRed maturation, we performed separate injections of AAV5.nlsGFP.Long and AAV2.dsRed.Long into the murine retina. At 5 weeks there was no red or green fluorescence in the retina injected with AAV2.dsRed.Long. GFP expression levels in photoreceptor cells in AAV5-injected eyes were comparable to those reported in Fig. 4 (data not shown).

Infection of AAV5.GFP.Short and AAV2.GFP.Short. We next compared levels of AAV5 and AAV2 transduction following injection of viruses expressing the same GFP transgene but containing half-length genomes. Subretinal injections of 7.5×10^8 particles of AAV5 or 1.2×10^9 particles of AAV2 were performed for between-eye comparisons. Animals were sacrificed, and eyes were evaluated 5 ($n = 4$ eyes per group)

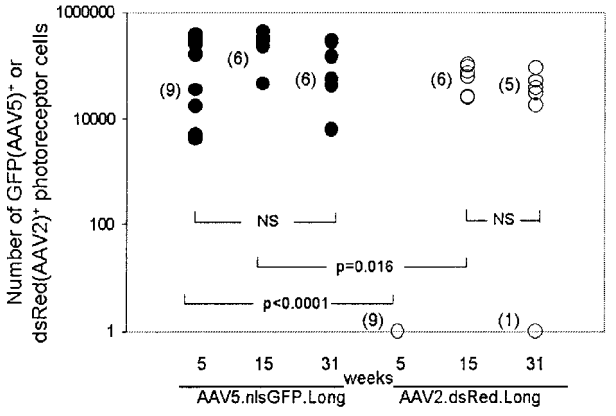

FIG. 4. Stereological assessment of transgene-positive cells in murine retina coinfected with AAV5.nlsGFP.Long and AAV2.dsRed.Long at 5, 15, and 31 weeks. Transgene-positive cells were determined as shown in Fig. 2 and as described in Materials and Methods. Numbers of eyes examined per group are given in parentheses. NS, not significant.

and 15 ($n = 9$ eyes per group) weeks after surgery. As seen in Fig. 6, GFP expression was detected in both RPE and photoreceptor cells for AAV2 and AAV5. Again, the time course for expression was faster with AAV5 than with AAV2 (Fig. 7). At 5 weeks, the mean number of transgene-positive photoreceptor cells was significantly higher in AAV5-injected eyes than in AAV2-injected eyes (250,000 ± 48,000 versus 62,000 ± 3,700; $P = 0.04$; Fig. 7). As was noted earlier, AAV5-mediated transgene expression was maintained from week 5 to 15, while there was a significant increase of expression of the AAV2 transgene from week 5 to 15 ($P < 0.0001$). The mean number of transgene-positive photoreceptor cells in AAV2-injected eyes was higher than the number in AAV5-injected eyes at 15 weeks (580,000 ± 40,000 versus 320,000 ± 21,000 cells; $P = 0.024$). AAV5.GFP.Short reached maximum expression levels of at week 5 and maintained the level of expression until week 15, similar to AAV5.GFP.Long.

Comparing half-length and wild-type-length genomes of AAV2. To further test if AAV2 transgene expression may be facilitated by a shortened genome length, we performed subretinal injections of 7.5×10^8 particles AAV2.GFP.Long (~4.8 kb) and 1.2×10^9 particles of AAV2.GFP.Short (~2.3 kb) in the murine retina. We found significantly greater numbers of transgene-positive photoreceptor cells in eyes injected with short genomes than in eyes injected with long genomes at weeks 5 (62,000 ± 3,700 versus 15.0 ± 10.0 cells; $P = 0.0003$) and 15 (580,000 ± 40,000 versus 1,000 ± 950.0 cells; $P = 0.018$), respectively (Fig. 8). The results remained significant when data from nonexpressing eyes were excluded (week 5: short genomes, 62,000 ± 3,700 cells; long genomes, 13,000 ± 2,100 cells; $P = 0.0069$; week 15: short genomes, 580,000 ± 40,000 cells; long genomes, 71,000 ± 11,000 cells; $P < 0.0001$). These results indicate that genome length can affect the efficiency of AAV2 transduction in murine photoreceptor cells, with the half-length genome achieving higher levels of transgene expression in a shorter amount of time and also maintaining higher levels of expression at 15 weeks than full-length genomes.

Comparison of infection of AAV2/5.GFP.Long and AAV2.GFP.Long. We next assessed the contribution of the capsid in AAV5-mediated gene transfer to photoreceptor cells. AAV2/5 (pseudotyped virus in which AAV2 genomes were packaged in AAV5 capsids) and AAV2 have the same transgene and ITRs but differ in capsid proteins. Subretinal injections of 1.2×10^9 particles of AAV2/5.GFP.Long and 7.5×10^8 particles AAV2.GFP.Long were performed. Mice were sacrificed 5 ($n = 10$ eyes per group) and 15 ($n = 8$ eyes for AAV2 and n = 10 eyes for AAV2/5) weeks after injection, and sections were observed for GFP fluorescence. GFP-positive photoreceptor cells and RPE cells were observed at both time points and for both viruses. Mean GFP expression of AAV2/5 was significantly higher than that of AAV2 at both 5 and 15 weeks (140,000 ± 82,000 versus 15.0 ± 10.0, $P = 0.0002$, at week 5; 400,000 ± 36,000 versus 1,000 ± 950.0, $P = 0.024$, at week 15) (Fig. 9). Group comparisons without the outliers also showed significant differences (540,000 ± 39,000 for AAV2/5 versus 13,000 ± 2,100 for AAV2, $P < 0.0001$, at week 5, and 400,000 ± 36,000 for AAV2/5 versus 71,000 ± 11,000 for AAV2, $P = 0.0008$, at week 15). There were no significant differences in AAV5 or AAV2 transgene expression from week 5 to 15. These results indicate that, in the context of a long genome, the AAV5 capsid is more efficient than the AAV2 capsid at transducing photoreceptor cells in the murine retina.

Quantification of viral genomes. The difference in the number of transgene-expressing photoreceptor cells may be due to differences in infection efficiency and/or due to differences in transgene expression following viral entry. Hirt DNA was harvested from retinas injected 14 weeks earlier with AAV2.GFP.Short (1.2×10^9 particles per eye), AAV2.GFP.Long (7.5×10^8 particles per eye), or AAV2/5.GFP.Long (1.2×10^9 particles per eye). As seen in Fig. 10, there were significantly more genome copies for AAV2/5.GFP.Long (450,000 ± 85,000 copies) than for AAV2.GFP.Long (16,000 ± 3,000 copies; $P = 0.0003$). Moreover, injections of AAV2.GFP.Short resulted in a 50-fold increase in genome copies (790,000 ± 120,000 copies;

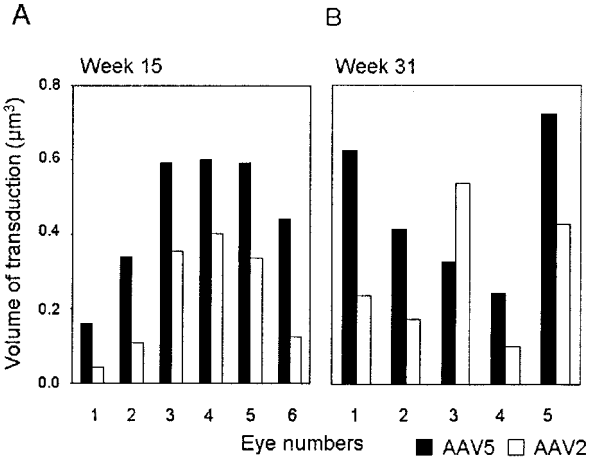

FIG. 5. Evaluation of transduction volume of murine retinas coinfected with AAV5.nlsGFP.Long and AAV2.dsRed.Long at 15 (A) and 31 (B) weeks. Serial sections of the entire eye were systematically sampled, and volumes were determined as described in Materials and Methods.

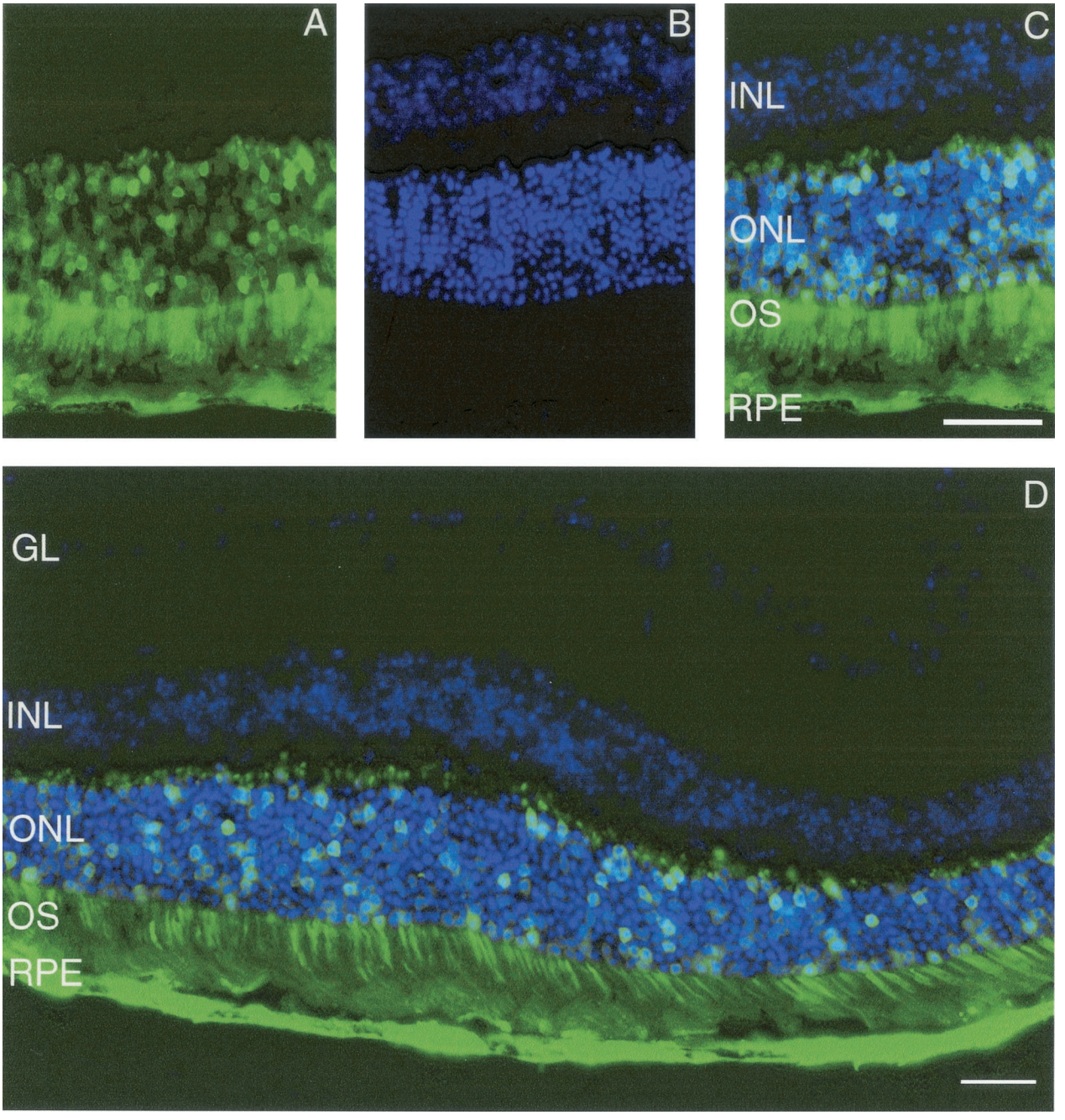

FIG. 6. Murine retinas infected with AAV5.GFP.Short 5 weeks after subretinal delivery. (A) GFP-positive RPE and photoreceptor cells (ONL and OS [outer segment]). (B) DAPI fluorescence depicting the nuclei within the ONL and INL. (C and D) Superimposed images demonstrating GFP-positive nuclei in the ONL. GL, ganglion layer. The photomicrographs are similar to those taken from retinas infected with AAV5.GFP.Short 15 weeks after injection and from retinas infected with AAV2.GFP.Short and AAV2/5.GFP.Long 5 and 15 weeks after surgery. Bars, 50 μm.

$P < 0.0001$) relative to the number produced by injections with AAV2.GFP.Long (Fig. 10).

Infection of pseudotyped AAV6 and AAV3 in the murine retina. Finally, we assessed the tissue tropism and transduction efficiency of AAV2/6 (AAV2 genome packaged in AAV6 capsid) and AAV2/3 (AAV2 genome packaged in AAV3 capsid) in the murine retina by performing subretinal injections. A solution of 5.7×10^7 particles of AAV2/6 or AAV2/3 was injected per eye, and animals were sacrificed 5 ($n = 6$ for both vectors) and 15 ($n = 6$ for both vectors) weeks after surgery. For AAV2/6, GFP was expressed in the RPE cells at both 5 and 15 weeks (Fig. 11). No other cell types were transduced. There was no transgene expression in the retina at 5 or 15 weeks for AAV2/3 injections.

DISCUSSION

We have shown that AAV2 and AAV5 can transduce photoreceptor and RPE cells and that AAV6 can transduce RPE

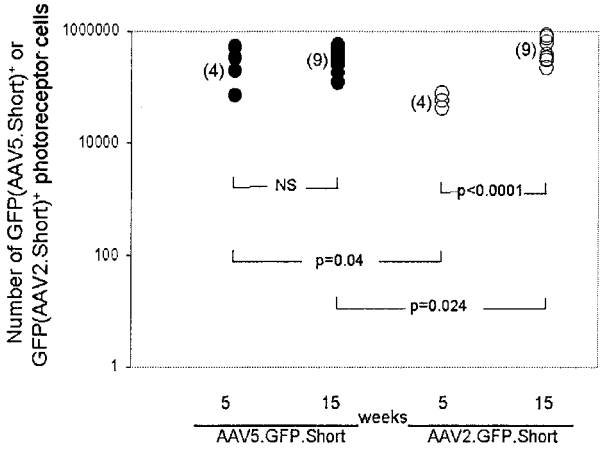

FIG. 7. Stereological assessment of transgene-positive cells in murine retinas infected with AAV5.GFP.Short and AAV2.GFP.Short at 5 and 15 weeks. NS, not significant.

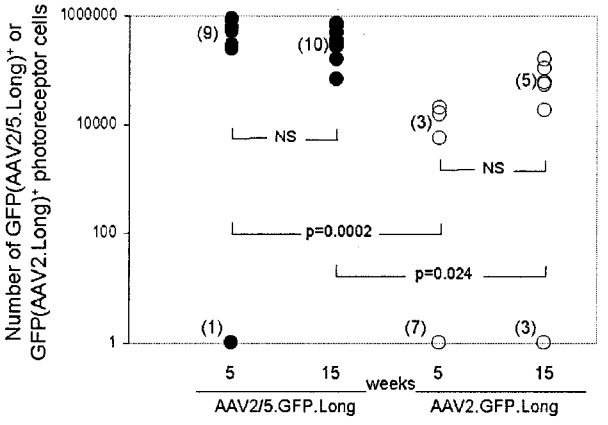

FIG. 9. Stereological assessment of transgene-positive cells in murine retinas infected with AAV2/5.GFP.Long and AAV2.GFP.Long at 5 and 15 weeks. NS, not significant.

cells in the murine retina. In general, we found that AAV5 had faster expression kinetics and led more transgene-positive cells and increased numbers of genome copies/retina relative to AAV2. We also observed persistent expression following gene transfer, up to 31 weeks in murine photoreceptor cells, a requirement for therapies of retinal degenerative diseases.

AAV2/6 holds promise for gene therapy of retinal degenerative disease due to specific mutations in the RPE. One example of this is Leber's congenital amaurosis (LCA), the earliest and most severe form of retinal degeneration. LCA is estimated to cause up to 10% of all congenital blindness in children (20). AAV2 and AAV5 also transduce RPE cells, but not specifically (1, 4, 5, 14, 15). While expression from AAV2- or AAV5-based vectors could be limited to expression in the RPE by specific promoters, it may be advantageous to utilize the natural tropism of the AAV6 capsid.

Transduction efficiency is dependent on initial viral binding and entry and various postentry processes, such as intracellular trafficking and second-strand synthesis. In comparisons of AAV2 with AAV3, -5, and -6, heterogeneities in the capsid-encoding regions, heparin binding assays, and different abilities to transduce cell lines in vitro all imply different receptor and coreceptor requirements for cell entry (7, 9, 18, 30, 40). While the receptors and coreceptors for AAV3 and -6 have not yet been defined, those for AAV2 include heparan sulfate proteoglycan, fibroblast growth factor receptor 1, and $\alpha_V\beta5$ integrins, whereas 2,3-linked sialic acid is a part of the receptor complex for AAV5 (29, 34–36, 40).

There is significant variation among the capsid proteins of the various AAV serotypes (7, 30). To evaluate the capsids' contribution to the tropism of AAV3, AAV5, and AAV6, subretinal injections of AAV2 genomes pseudotyped into these respective capsids were done and gene transfer was quantified. We showed that AAV2/3 does not transduce cells in the murine retina, probably because the murine retina does not have the necessary receptor and coreceptor for AAV3 capsid binding. Though it is possible that the lack in gene transfer noted by AAV3 is dosage dependent, the doses administered were similar to those of AAV2.dsRed.Long and

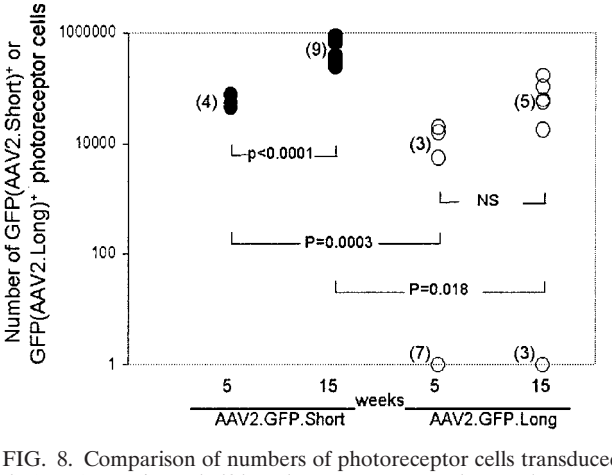

FIG. 8. Comparison of numbers of photoreceptor cells transduced with AAV2 carrying a half-length genome versus the number transduced with AAV2 carrying a wild-type length genome (see Fig. 1). NS, not significant.

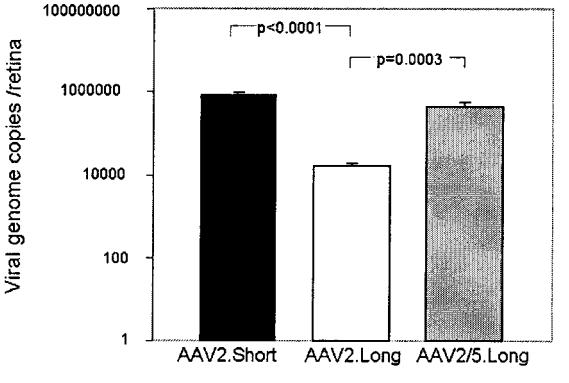

FIG. 10. Quantification of viral genomes extracted from murine retinas 14 weeks after subretinal delivery of AAV2/5.GFP.Long, AAV2.GFP.Long, and AAV2.GFP.Short using real-time PCR.

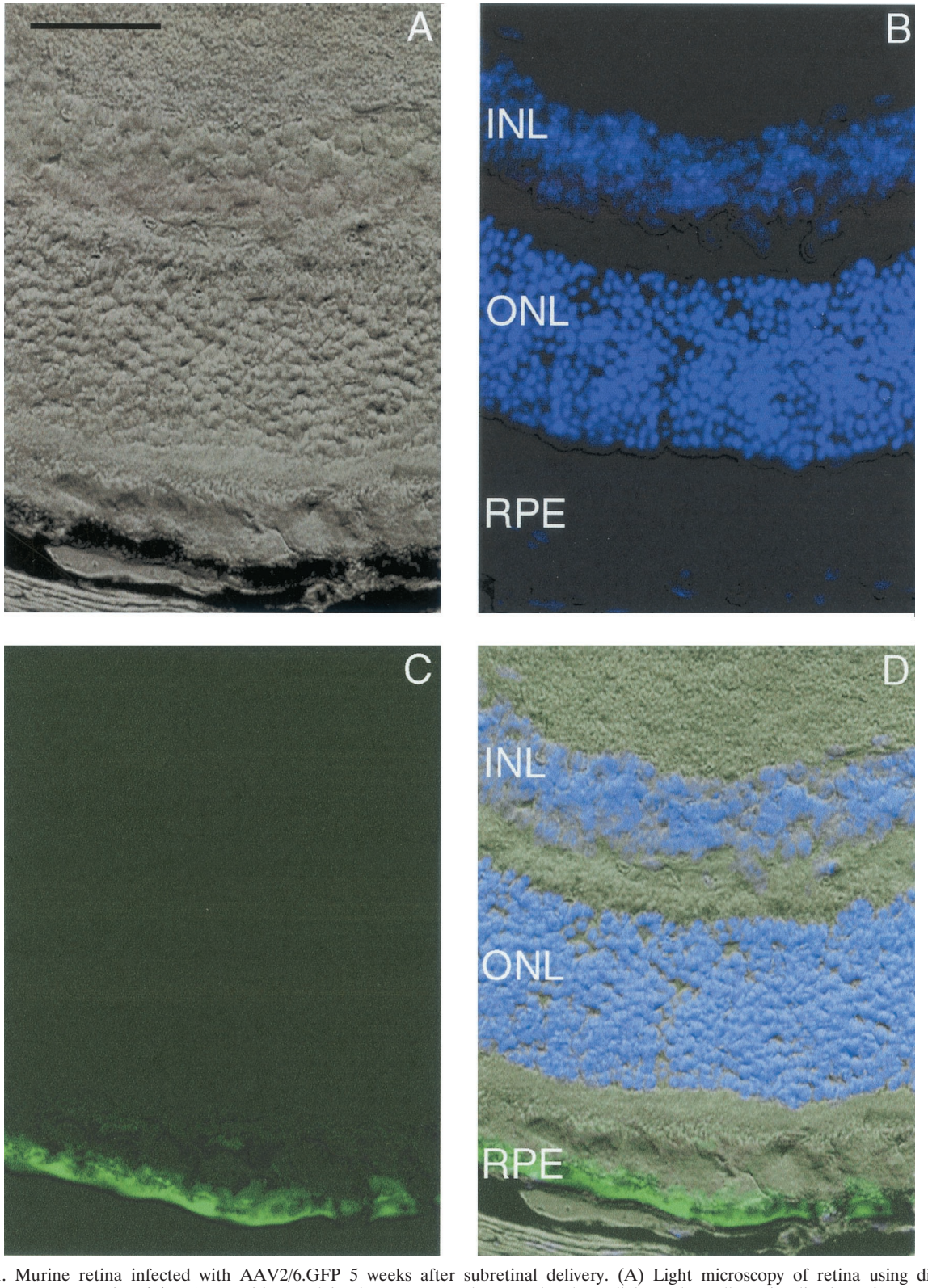

FIG. 11. Murine retina infected with AAV2/6.GFP 5 weeks after subretinal delivery. (A) Light microscopy of retina using differential interference contrast optics. (B) DAPI-positive nuclei. The area near the RPE has been lightened to allow visualization of DAPI staining. (C) GFP-positive RPE. (D) Superimposed images of panels A to C. Photomicrographs are similar to those taken from retinas harvested 15 weeks after surgery. Bar, 50 μm.

AAV5.nlsGFP.Long. Also, a similar dose of AAV2/6 resulted in transduction of RPE cells.

Our data are consistent with those of Auricchio et al., in which AAV2/1 (similar to AAV2/6) was found to transduce mostly RPE, with limited gene transfer to photoreceptor cells, Müller cells, and cells in the inner nuclear layer (2). The fact that we did not find other retinal cells transduced may be due to the lower dosage used in each eye (10^7 versus 10^9 genome copies per eye) or the promoter (CMV enhancer and chicken β-actin versus CMV enhancer and promoter). While the stability of the expression of AAV2/1 was not previously reported, in our study eyes injected with AAV2/6 showed stable expression out to 15 weeks.

AAV2/5 and AAV2 were able to transduce photoreceptor and RPE cells. For vectors containing full-length genomes, AAV2/5 was much more efficient at transducing photoreceptor cells in the murine retina than AAV2 at all time points. We found a 400-fold increase in the number of transgene-expressing cells with AAV2/5 and 30-fold more genome copies of AAV2/5 than of AAV2 15 weeks after injection. The contribution of the AAV5 capsid, relative to that of AAV2, is therefore significant in enhancing transgene expression in murine photoreceptor cells.

Our data suggest that, in the retina, the binding of the AAV capsids to the cell is not the sole determinant of transduction efficiency. We found that AAV2 transgene expression could be enhanced by reduction in genome length. The requirement of a complementary strand for the single-stranded AAV DNA to become transcriptionally active is considered to be a limiting factor for AAV transduction (26). AAV may rely on host cellular replication factors for synthesis of the complementary strand. The ITRs at AAV termini are palindromic and allow for host DNA polymerase-mediated second-strand synthesis. It has been shown that AAV DNA of less than one-half the wild-type-AAV length can be packaged as a dimer, with the dimeric DNA molecules in an inverted-repeat configuration (26). These self-complementary molecules may refold into double-stranded DNA templates for expression. This may bypass the need for synthesis or recruitment or allow for increased stability. McCarty et al. showed that half-length AAV was greater than fourfold more efficient than monomeric genomes in gene transfer to cultured HeLa cells (26). Our studies showed that vectors containing the AAV2 short genomes mediate five- and eightfold-greater transgene expression than wild-type-length AAV2 genomes at 5 and 15 weeks, respectively. Moreover, we found a 50-fold increase in half-length viral AAV2 genomes relative to the wild type in eyes harvested 14 weeks after injection.

Numerous reports have shown that the lack of AAV2 transgene expression in various tissues can be due to postentry processes. AAV2 vectors efficiently internalize from the apical surface of differentiated human airway epithelia but achieve poor transgene expression, in part due to ubiquitination of the AAV capsid after virion internalization and endosomal release (13). In differentiated myocytes, AAV2 has been shown to provide for poorer transduction than AAV5 despite higher binding efficiency (12). In the eye, Flannery and colleagues showed that AAV2-mediated murine photoreceptor cell transduction could be improved by replacing the CMV promoter with the rod opsin promoter, indicating that expression, rather than viral entry, was limiting (14).

In previous reports, transduction efficiency has been evaluated by selecting a few representative sections from the most successfully transduced eyes and estimating the area of transgene expression (2, 27). Some investigators estimated the area of GFP-positive photoreceptor cells by in vivo indirect opthalmoscopy, epifluorescence images of retinal whole mounts, or serial confocal images of the region directly adjacent to the injection site (2, 14). In contrast, the stereological approach used in this study allows for the quantification of the total number of transduced photoreceptors. Systematic random sampling of the entire tissue of interest reduces the large variation observed in sampling (28). This is especially important when comparing the transduction efficiencies of various viral vectors.

Most retinal degenerative diseases are caused by mutations in genes expressed in photoreceptor cells (10). It is estimated that the mouse retina contains approximately 180,000 cones and 6.4 million rods (22). By using stereological analysis, we estimate that AAV5 can transduce up to 15% of photoreceptor cells. While half-length AAV2 and AAV5 can transduce similar numbers of photoreceptor cells at 15 weeks, the size limitation of half-length AAV2 may make it impractical for many disease applications.

In summary, we have quantitatively defined the kinetics and efficiency of AAV transduction of photoreceptor cells. Our data suggest that genome length and AAV capsids can be used to fine tune delivery and expression kinetics to specific cells within the retina. These features will become important to retinal gene therapy as the underlying bases of retinal diseases are elucidated.

ACKNOWLEDGMENTS

We thank Dongshen Duan for critical discussions, Shawn Roach for graphic art, Bridget Zimmerman for statistical support, and Christine McLennan for manuscript assistance.

This work was supported by the NIH (grants HL58340, DK54759, HD33531, and DC00040) and the Roy J. Carver Trust (B.L.D.).

REFERENCES

1. **Ali, R. R., M. B. Reichel, M. De Alwis, N. Kanuga, C. Kinnon, R. J. Levinsky, D. M. Hunt, S. S. Bhattacharya, and A. J. Thrasher.** 1998. Adeno-associated virus gene transfer to mouse retina. Hum. Gene Ther. **9:**81–86.
2. **Auricchio, A., G. Kobinger, V. Anand, M. Hildinger, E. O'Connor, A. M. Maguire, J. M. Wilson, and J. Bennett.** 2001. Exchange of surface proteins impacts on viral vector cellular specificity and transduction characteristics: the retina as a model. Hum. Mol. Genet. **10(26):**3075–3081.
3. **Baird, G. S., D. A. Zacharias, and R. Y. Tsien.** 2000. Biochemistry, mutagenesis, and oligomerization of DsRed, a red fluorescent protein from coral. Proc. Natl. Acad. Sci. USA **97:**11984–11989.
4. **Bennett, J., D. Duan, J. F. Engelhardt, and A. M. Maguire.** 1997. Real-time, noninvasive in vivo assessment of adeno-associated virus-mediated retinal transduction. Investig. Ophthalmol. Vis. Sci. **38:**2857–2863.
5. **Bennett, J., A. M. Maguire, A. V. Cideciyan, M. Schnell, E. Glover, V. Anand, T. S. Aleman, N. Chirmule, A. R. Gupta, Y. Huang, G.-P. Gao, W. C. Nyberg, J. Tazelaar, J. Hughes, J. M. Wilson, and S. G. Jacobson.** 1999. Stable transgene expression in rod photoreceptors after recombinant adeno-associated virus-mediated gene transfer to monkey retina. Proc. Natl. Acad. Sci. USA **96:**9920–9925.
6. **Chiorini, J. A., S. Afione, and R. M. Kotin.** 1999. Adeno-associated virus (AAV) type 5 Rep protein cleaves a unique terminal resolution site compared with other AAV serotypes. J. Virol. **73:**4293–4298.
7. **Chiorini, J. A., F. Kim, L. Yang, and R. M. Kotin.** 1999. Cloning and characterization of adeno-associated virus type 5. J. Virol. **73:**1309–1319.
8. **Chiorini, J. A., C. M. Wendtner, E. Urcelay, B. Safer, M. Hallek, and R. M. Kotin.** 1995. High-efficiency transfer of the T cell co-stimulatory molecule B7–2 to lymphoid cells using high-titer recombinant adeno-associated virus vectors. Hum. Gene Ther. **6:**1531–1541.

9. **Davidson, B. L., C. S. Stein, J. A. Heth, I. Martins, R. M. Kotin, T. A. Derksen, J. Zabner, A. Ghodsi, and J. A. Chiorini.** 2000. Recombinant AAV type 2, 4 and 5 vectors: transduction of variant cell types and regions in the mammalian CNS. Proc. Natl. Acad. Sci. USA **97:**3428–3432.
10. **Dryja, T. P., and T. Li.** 1995. Molecular genetics of retinitis pigmentosa. Hum. Mol. Genet. **4:**1739–1743.
11. **Duan, D., P. Sharma, J. Yang, Y. Yue, L. Dudus, Y. Zhang, K. J. Fisher, and J. F. Engelhardt.** 1998. Circular intermediates of recombinant adeno-associated virus have defined structural characteristics responsible for long-term episomal persistence in muscle tissue. J. Virol. **72:**8568–8577.
12. **Duan, D., Z. Yan, Y. Yue, W. Ding, and J. F. Engelhardt.** 2001. Enhancement of muscle gene delivery with pseudotyped adeno-associated virus type 5 correlates with myoblast differentiation. J. Virol. **75:**7662–7671.
13. **Duan, D., Y. Yue, Z. Yan, J. Yang, and J. F. Engelhardt.** 2000. Endosomal processing limits gene transfer to polarized airway epithelia by adeno-associated virus. J. Clin. Investig. **105:**1573–1587.
14. **Flannery, J. G., S. Zolotukhin, M. I. Vaquero, M. M. LaVail, N. Muzyczka, and W. W. Hauswirth.** 1997. Efficient photoreceptor-targeted gene expression in vivo by recombinant adeno-associated virus. Proc. Natl. Acad. Sci. USA **94:**6916–6921.
15. **Grant, C. A., S. Ponnazhagan, X.-S. Wang, A. Srivastava, and T. Li.** 1997. Evaluation of recombinant adeno-associated virus as a gene transfer vector for the retina. Curr. Eye Res. **16:**949–956.
16. **Grimm, D., A. Kern, K. Rittner, and J. A. Kleinschmidt.** 1998. Novel tools for production and purification of recombinant adeno-associated virus vectors. Hum. Gene Ther. **9:**2745–2760.
17. **Gundersen, H. J. G., and E. B. Jensen.** 1987. The efficiency of systematic sampling in sterology and its prediction. J. Microsc. **147:**229–263.
18. **Halbert, C. L., J. M. Allen, and A. D. Miller.** 2001. Adeno-associated virus type 6 (AAV6) vectors mediate efficient transduction of airway epithelial cells in mouse lungs compared to that of AAV2 vectors. J. Virol. **75:**6615–6624.
19. **Halbert, C. L., E. A. Rutledge, J. M. Allen, D. W. Russell, and D. Miller.** 2000. Repeat transduction in the mouse lung by using adeno-associated virus vectors with different serotypes. J. Virol. **74:**1524–1532.
20. **Harris, E. W.** 2001. Leber's congenital amaurosis and RPE65. Int. Ophthalmol. Clin. **41:**73–82.
21. **Hildinger, M., A. Auricchio, G. Gao, L. Wang, N. Chirmule, and J. M. Wilson.** 2001. Hybrid vectors based on adeno-associated virus serotypes 2 and 5 for muscle-directed gene transfer. J. Virol. **75:**6199–6203.
22. **Jeon, C. J., E. Strettoi, and R. H. Masland.** 1998. The major cell populations of the mouse retina. J. Neurosci. **18:**8936–8946.
23. **Klein, R. L., E. M. Meyer, A. L. Peel, S. Zolotukhin, C. Meyers, N. Muzyczka, and M. A. King.** 1998. Neuron-specific transduction in the rat septohippocampal or nigrostriatal pathway by recombinant adeno-associated virus vectors. Exp. Neurol. **150:**183–194.
24. **Laughlin, C. A., J. D. Tratschin, H. Coon, and B. J. Carter.** 1983. Cloning of infectious adeno-associated virus genomes in bacterial plasmids. Gene **23:** 65–73.
25. **Lewin, A. S., K. A. Drenser, W. W. Hauswirth, S. Nishikawa, D. Yasumura, J. G. Flannery, and M. A. LaVail.** 1998. Ribozyme rescue of photoreceptor cells in a transgenic rat model of autosomal dominant retinitis pigmentosa. Nat. Med. **4:**967–971.
26. **McCarty, D. M., P. E. Monahan, and R. J. Samulski.** 2001. Self-complementary recombinant adeno-associated virus (scAAV) vectors promote efficient transduction independently of DNA synthesis. Gene Ther. **8:**1248–1254.
27. **Miyoshi, H., M. Takahaski, F. H. Gage, and I. M. Verma.** 1997. Stable and efficient gene transfer into the retina using an HIV-based lentiviral vector. Proc. Natl. Acad. Sci. USA **94:**10319–10323.
28. **Mohand-Said, S., A. Deudon-Combe, D. Hicks, M. Simonutti, V. Forster, A. C. Fintz, T. Leveillard, H. Dreyfus, and J. A. Sahel.** 1998. Normal retina releases a diffusible factor stimulating cone survival in the retinal degeneration mouse. Proc. Natl. Acad. Sci. USA **95:**8357–8362.
29. **Qing, K., C. Mah, J. Hansen, S. Zhou, V. Dwarki, and A. Srivastava.** 1999. Human fibroblast growth factor receptor 1 is a co-receptor for infection by adeno-associated virus 2. Nat. Med. **5:**71–77.
30. **Rutledge, E. A., C. L. Halbert, and D. W. Russell.** 1998. Infectious clones and vectors derived from adeno-associated virus (AAV) serotypes other than AAV type 2. J. Virol. **72:**309–319.
31. **Samulski, R. J., L. S. Chang, and T. Shenk.** 1989. Helper-free stocks of recombinant adeno-associated viruses: normal integration does not require viral gene expression. J. Virol. **63:**3822–3828.
32. **Schmidt, M., S. Afione, and R. M. Kotin.** 2000. Adeno-associated virus type 2 rep78 induces apoptosis through caspase activation independently of p53. J. Virol. **74:**9441–9450.
33. **Smith, R. H., S. Afione, and R. M. Kotin.** Transposase-mediated construction of an integrated adeno-associated virus type 5 helper plasmid. BioTechniques, in press.
34. **Summerford, C., J. S. Bartlett, and R. J. Samulski.** 1999. αvβ5 integrin: a co-receptor for adeno-associated virus type 2 infection. Nat. Med. **5:**78–82.
35. **Summerford, C., and R. J. Samulski.** 1998. Membrane-associated heparan sulfate proteoglycan is a receptor for adeno-associated virus type 2 virions. J. Virol. **72:**1438–1445.
36. **Walters, R. W., S. Yi, S. Keshavjee, K. E. Brown, M. J. Welsh, J. A. Chiorini, and J. Zabner.** 2001. Binding of adeno-associated virus type 5 to 2,3-linked sialic acid is required for gene transfer. J. Biol. Chem. **276:**20610–20616.
37. **Xiao, W., N. Chirmule, S. C. Berta, B. McCullough, G. Gao, and J. M. Wilson.** 1999. Gene therapy vectors based on adeno-associated virus type 1. J. Virol. **73:**3994–4003.
38. **Yan, Z., T. C. Ritchie, D. Duan, and J. F. Engelhardt.** 2002. Recombinant AAV-mediated gene delivery using dual vector heterodimerization. Methods Enzymol. **346:**334–357.
39. **Yan, Z., R. Zak, G. W. G. Luxton, T. C. Ritchie, U. Bantel-Schaal, and J. F. Engelhardt.** 2002. Ubiquitination of both adeno-associated virus type 2 and 5 capsid proteins affects the transduction efficiency of recombinant vectors. J. Virol. **76:**2043–2053.
40. **Zabner, J., M. Seiler, R. Walters, R. M. Kotin, W. Fulgerus, B. L. Davidson, and J. A. Chiorini.** 2000. Adeno-associated virus type 5 (AAV5) but not AAV2 binds to the apical surfaces of airway epithelia and facilitates gene transfer. J. Virol. **74:**3852–3858.